ment of actomyosin contractility. mDia recruits profilin (*20*), likely promoting actin polymerization (*21*). These pathways thus may underlie neurite retraction as well as other Rho-mediated processes such as stress fiber formation (*2*). Rac, another member of the Rho family of GTPases, induces membrane ruffles and also activates LIM-kinase and triggers the phosphorylation of cofilin (*17*), but reduces actomyosin-based contractility (*22*). These observations suggest that Rho and Rac combine the same mechanism—inactivation of cofilin—differently with other mechanisms to produce different phenotypes. The observation that only a limited amount of cofilin is phosphorylated in response to cell stimulation (Fig. 1B) suggests that this mechanism may not influence the behavior of actin filaments throughout the cell; however, it certainly contributes to the temporal and spatial reorganization of specific actin cytoskeletons by the Rho family GTPases.

References and Notes

1. M. D. Welch, A. Mallavarapu, J. Rosenblatt, T. J. Mitchison, *Curr. Opin. Cell Biol.* **9**, 54 (1997).
2. S. Narumiya, *J. Biochem. (Tokyo)* **120**, 215 (1996); A. Hall, *Science* **279**, 509 (1998).
3. K. Kimura *et al.*, *Science* **273**, 245 (1996).
4. K. Burridge, M. Chrzanowska-Wodnicka, C. Zhong, *Trends Cell Biol.* **7**, 342 (1997).
5. M. Uehata *et al.*, *Nature* **389**, 990 (1997).
6. K. Kimura *et al.*, *J. Biol. Chem.* **273**, 5542 (1998); T. Matsui *et al.*, *J. Cell Biol.* **140**, 647 (1998).
7. K. Jalink *et al.*, *J. Cell. Biol.* **126**, 801 (1994).
8. M. Hirose *et al.*, *ibid.* **141**, 1625 (1998).
9. After LPA stimulation, N1E-115 cells were lysed with 10 mM tris-HCl (pH 7.5) containing 1 mM EGTA, 5 mM $MgCl_2$, 1 mM dithiothreitol, 1% (v/v) Triton X-100, and mixtures of phosphatase inhibitors and protease inhibitors. Lysates were centrifuged, and the supernatant, corresponding to 2×10^4 cells, was subjected to two-dimensional electrophoresis with a linear pH gradient from 3.5 to 10, followed by autoradiography.
10. Purification and identification details of P1 and P2 proteins are available at www.sciencemag.org/feature/data/1041678.shl.
11. A. Moon and D. G. Drubin, *Mol. Biol. Cell* **6**, 1423 (1995).
12. S. Ono, N. Monami, H. Abe, T. Obinata, *J. Biol. Chem.* **269**, 15280 (1994).
13. In the transfection experiments in this study, COS-7 cells were transfected with combinations of the following vectors: pFL-C1-FLAG–tagged wild-type (WT) or S3A cofilin, pCAG-Myc–tagged ROCKΔ1 (*14*), pUCD2-SRα-FLAG–tagged LIMK1 (*17*), pUC-SRα-Myc–tagged LIMK 2 [I. Okano *et al.*, *J. Biol. Chem.* **270**, 31321 (1995)], pCMV5-FLAG–tagged N^{17}-Rac (*8*), pEXV-Myc–tagged V^{14}-Rho (*14*), and pCAG-Myc–tagged ROCK-KDIA (*14*). After transfection, cells were cultured for 15 hours in Dulbecco's minimum essential medium containing 10% fetal bovine serum (Fig. 1C) or in serum-free OPTI-MEM (Gibco) (Figs. 2B and 3A). In the experiments in Figs. 1C and 3A, the cells were then labeled for 4 hours with [^{32}P]orthophosphate (50 μCi/ml). Cells were lysed in 20 mM tris-HCl (pH 7.5) containing 1 mM EDTA, 1 mM EGTA, 5 mM $MgCl_2$, 5 mM 2-mercaptoethanol, 0.05% Triton X-100, and mixtures of phosphatase inhibitors and protease inhibitors. FLAG-tagged cofilin was immunoprecipitated with anti-FLAG (M2) affinity beads (Sigma) and subjected to SDS–polyacrylamide gel electrophoresis (SDS-PAGE) followed by autoradiography or immunoblot analysis (Figs. 1C and 3A). FLAG-tagged LIMK1 was immunoprecipitated and subjected to kinase assay (*16*) (Fig. 2B).
14. T. Ishizaki *et al.*, *FEBS Lett.* **404**, 118 (1997).
15. T. E. Morgan *et al.*, *J. Cell Biol.* **122**, 623 (1993); B. J. Agnew, L. S. Minamide, J. R. Bamburg, *J. Biol. Chem.* **270**, 17582 (1995); K. Moriyama *et al.*, *Genes Cell* **1**, 73 (1996).
16. His_6-tagged cofilin was expressed in *Escherichia coli* and His_6-tagged ROCKΔ4 (residues 1 to 477) was produced in Sf9 cells. Kinase reactions were done in a total volume of 23 μl at 30°C for 10 min with 50 μM [γ-^{32}P]ATP (adenosine 5′-triphosphate) and 4 μg of either cofilin or histone type 2 as substrates in kinase buffer [25 mM Hepes-NaOH (pH 7.5), 10 mM $MgCl_2$, 5 mM $MnCl_2$, 0.1 mM EGTA, 0.05% Brij 35, 5 mM 2-mercaptoethanol, phosphatase inhibitors, and protease inhibitors].
17. S. Arber *et al.*, *Nature* **393**, 805 (1998); N. Yang *et al.*, *ibid.*, p. 809.
18. M. Maekawa *et al.*, unpublished data.
19. P. Lappalanien and D. G. Drubin, *Nature* **388**, 78 (1997); M.-F. Carlier *et al.*, *J. Cell Biol.* **136**, 1307 (1997).
20. N. Watanabe *et al.*, *EMBO J.* **16**, 1307 (1997).
21. D. Pantaloni and M.-F. Carlier, *Cell* **75**, 1007 (1993).
22. L. C. Sanders, F. Matsumura, G. M. Bokoch, P. de Lanerolle, *Science* **283**, 2083 (1999).

23. Supported by grants from the Ministry of Education, Science and Culture of Japan and from the Human Frontier Science Program. We thank E. Nishida, I. Yahara, and T. Doi for advice, and A. Shinohara for mass spectrometry. M.M. thanks S. Maekawa for encouragement.

11 May 1999; accepted 1 July 1999

Fas Ligand: A Sensor for DNA Damage Critical in Skin Cancer Etiology

Laurie L. Hill, Allal Ouhtit, Susan M. Loughlin, Margaret L. Kripke, Honnavara N. Ananthaswamy, Laurie B. Owen-Schaub*

DNA-damaged cells can either repair the DNA or be eliminated through a homeostatic control mechanism termed "cellular proofreading." Elimination of DNA-damaged cells after ultraviolet radiation (UVR) through sunburn cell (apoptotic keratinocyte) formation is thought to be pivotal for the removal of precancerous skin cells. Sunburn cell formation was found to be dependent on Fas ligand (FasL), a pro-apoptotic protein induced by DNA damage. Chronic exposure to UVR caused 14 of 20 (70 percent) FasL-deficient mice and 1 of 20 (5 percent) wild-type mice to accumulate p53 mutations in the epidermis. Thus, FasL-mediated apoptosis is important for skin homeostasis, suggesting that the dysregulation of Fas-FasL interactions may be central to the development of skin cancer.

In the United States, nearly 1,000,000 persons will develop nonmelanoma skin cancer (NMSC) (basal and squamous cell carcinoma) this year. Although death from NMSC is rare, these patients experience a substantially increased mortality from other cancers (20 to 30% higher), suggesting that skin cancer susceptibility may be linked to the development of noncutaneous malignancies (*1*). UVR in sunlight is the principal carcinogen, serving as initiator and promoter for most skin tumors (*2*). UVR elicits p53-dependent apoptosis in DNA-damaged keratinocytes (sunburn cells), presumably as a "guardian of the tissue" response to eradicate precancerous cells in the skin (*3*). This p53-driven response, termed "cellular proofreading" (*3*), erases rather than repairs DNA damage. Mice deficient in p53 (p53-null) have reduced sunburn cell formation and increased susceptibility to UVR-induced skin carcinogenesis (*2*, *4*), implicating apoptosis as a critical event in skin carcinogenesis. Fas and FasL are complementary receptor-ligand proteins eliciting apoptosis (*5*). Although Fas and FasL are induced by nuclear factor kappa B activation (*6*–*8*), wild-type p53 is essential for the transcriptional up-regulation of Fas after DNA damage (*9*–*11*). Thus, Fas and FasL may serve as external pro-apoptotic sensors of DNA damage–mediated cellular proofreading.

To investigate Fas and FasL expression in normal skin after UVR, we shaved C3H/HeJ wild-type mice, exposed them to a single dose of ultraviolet (UV) light (5 kJ/m^2) (*12*), and harvested epidermal skin sections for immunohistochemistry (*13*). Nonirradiated skin had little Fas and FasL expression (Fig. 1). Both Fas and FasL expression were potently induced in the epidermis by UVR as early as 3 and 6 hours after irradiation, with maximal induction of both proteins occurring at 12 hours. By 24 hours, UVR-induced Fas and FasL expression in the epidermis was similar to that observed before treatment. Dermal Fas expression (hair follicles and sebaceous glands), in contrast, remained elevated at this time point. These results indicate that both Fas and FasL are transiently up-regulated only in the normal epidermis by UVR exposure, as previously reported in human skin (*8*).

Because the proapoptotic proteins Fas and

Department of Immunology, University of Texas, M. D. Anderson Cancer Center, Houston, TX 77030, USA.

*To whom correspondence should be addressed. E-mail: lowensch@mdanderson.org

FasL are coexpressed in the UVR-exposed epidermis, we examined C3H/HeJ wild-type and FasL-deficient (C3H/HeJ *gld/gld*) mice 24 hours after exposure to UVR (5 kJ/m^2) to determine if the number of apoptotic keratinocytes was reduced (*14*). Typically, sunburn cells display a characteristic morphology of pycnotic nuclei and intensely eosinophilic cytoplasm detectable by light microscopy in hematoxylin-eosin–stained epidermal sections. Epidermal sections from UVR-treated wild-type mice had an average of 65.2 ± 17.3 (mean ± SE) sunburn cells per linear centimeter (Table 1), whereas epidermal sections from UVR-exposed FasL-deficient mice showed only 18.0 ± 9.3 sunburn cells per linear centimeter ($P < 0.001$, student's t test). The apoptotic nature of the sunburn cells identified by morphologic evaluation was confirmed by in situ TdT-mediated deoxyuridine triphosphate nick end labeling (TUNEL) (*15*). Few apoptotic cells were observed in the nonirradiated skin of either wild-type or FasL-deficient (*gld/gld*) mice (Fig. 2). In concert with our results using hematoxylin-eosin–stained epidermal sections, numerous apoptotic cells were detectable in wild-type, but not FasL-deficient, mice after UVR exposure. The reduction in sunburn cell formation in FasL-deficient mice was not attributable to kinetic differences in keratinocyte apoptosis because *gld/gld* mice had similar incidences in sunburn cell formation at 12, 24, and 48 hours after UVR exposure (*16*). Proliferative cell nuclear antigen expression in the epidermis was indistinguishable in wild-type and *gld/gld* mice 24 hours after UV-B exposure, making it unlikely that differences in UVR-induced keratinocyte apoptosis were attributable to differences in the epidermal proliferative responses (*17*). The contribution of T cells to this process also appears to be negligible as T cell–deficient mice (RAG 2$^{-/-}$) demonstrate UVR-induced sunburn cell responses similar to those of their wild-type counterparts (*18*). Furthermore, p53 localized to the nucleus and induced the downstream effector p21 (*waf1/cip1*) in both wild-type and FasL-deficient mice treated with UVR (*16*), suggesting that repression of p53 activation and function is not likely to contribute to the observed reduction in sunburn cells. Thus, UVR-induced sunburn cell formation requires Fas and FasL interactions, and p53 activation alone is insufficient to induce wild-type levels of apoptosis in UVR-damaged keratinocytes.

Table 1. Sunburn cell formation in wild-type and *gld* mice.

Strain (*N*)	UV-B (5 kJ/m^2)	Sunburn cells (*N*) ± SE*
C3H/HeJ (2)	−	0 ± 4
C3H/HeJ (4)	+	65.2 ± 17.3
C3H/*gld* (3)	−	0 ± 4
C3H/*gld* (5)	+	18.0 ± 9.3

*Numbers given are per linear centimeter and represent normalized values against sunburn cells in nonirradiated controls.

The elimination of cells sustaining extensive DNA damage has been proposed as a mechanism to avoid propagation of cells constituting a neoplastic risk (*3*). In the event that cellular proofreading is hindered, mutations in critical genes regulating cellular proliferation, adhesion, and apoptosis would be expected to accumulate upon exposure to DNA-damaging agents. To test the premise that FasL-induced apoptosis restricts the accumulation of genetic mutations after DNA damage, we examined epidermal sheets from *gld/gld* and wild-type mice for mutations in p53, a gene known to play a central role in UVR-induced, nonmelanoma skin carcinogenesis (Fig. 3). In contrast to the high frequency of mutant p53 alleles in tumor tissues, the frequency of p53 mutations in UV-irradiated skin is low because only a small fraction of the cells in the epidermis are mutated (*19*). Thus, detection of p53 mutations in UVR-exposed skin by conventional procedures is difficult. We used a sensitive allele-specific polymerase chain reaction (PCR) technique to detect p53 mutations (C → T transitions) at codons 270 and 275 because these codons are hotspots in UVR-induced mouse skin tumors (*20*, *21*). Mice were chronically irradiated on shaved dorsal skin for 1 and 2 weeks, representing five and ten exposures to UV-B (5 kJ/m^2), respectively (*22*). Two days after the final UVR exposure, epidermal sheets were harvested from 10 mice per group (with the exception of nonirradiated *gld/gld* mice, of which only nine mice were analyzed), and DNA was extracted. Mice were individually analyzed for p53 mutations in both codons 270 and 275, and the relative incidence was determined (Fig. 3B). Although only 1 of 20 wild-type mice showed evidence of p53 mutation after 1 or 2 weeks of chronic UVR exposure (codon 275), abundant p53 mutations were observed in FasL-deficient mice after only 1 week of UVR exposure (Fig. 3A). p53 mutations at

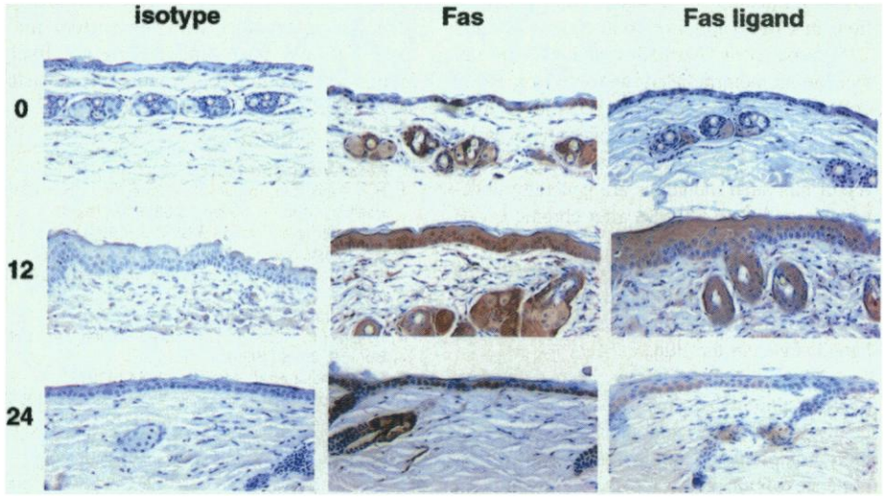

Fig. 1. Fas and FasL in skin after UVR exposure. Wild-type mice were acutely exposed to UV-B light (5 kJ/m^2), skin samples were harvested at indicated times (hours) after UVR exposure, and immunohistochemistry was performed (*13*). Sections are representative of a minimum of four mice examined at each time point. Magnification, ×10.

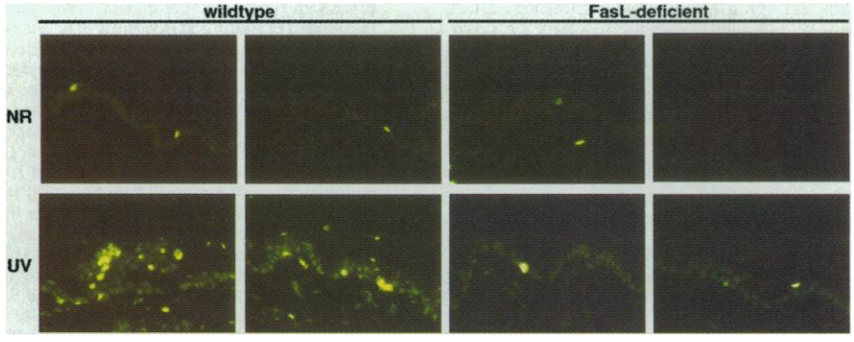

Fig. 2. Sunburn cell induction in wild-type and FasL-deficient (*gld/gld*) mice after UVR. Mice were acutely exposed to UV-B light (5 kJ/m^2), and skin sections were harvested for TUNEL analysis at 0 (NR) and 24 (UV) hours (*15*). A minimum of four mice (nonirradiated and irradiated) were examined; sections from two individual mice are shown. NR, nonirradiated. Magnification, ×10.

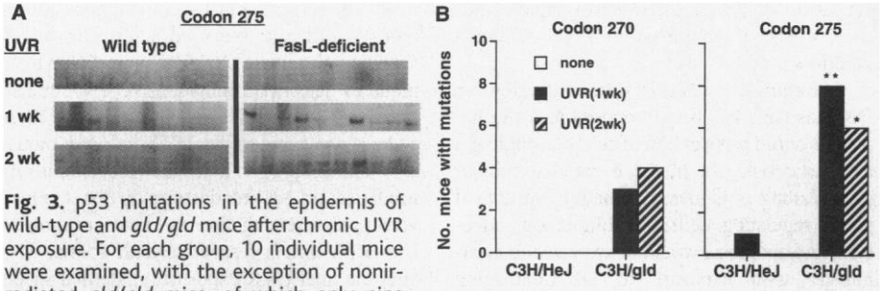

Fig. 3. p53 mutations in the epidermis of wild-type and *gld/gld* mice after chronic UVR exposure. For each group, 10 individual mice were examined, with the exception of nonirradiated *gld/gld* mice, of which only nine mice were examined. (**A**) Autoradiographs for codon 275 at the indicated type points. Each lane represents the analysis of an individual mouse. Bands indicate the presence of the C → T mutation in the codon. Mutations are present in wild-type mice only in lane 3 at week 1; *gld/gld* mice show mutations in lanes 1, 3 to 5, and 7 to 10 at week 1 and lanes 4 to 9 at week 2. (**B**) Graphic representation of mutation incidence. An unconditional exact two-sided *P* value was computed with the unconditional exact confidence interval of 95% for the difference of proportions (StatXact-3, V3.0.2; Cytel Software, Cambridge, MA) to determine statistical significance between wild-type and *gld/gld* mice at each time point for each codon. **, $P = 0.0046$; *, $P = 0.014$.

codons 270 and 275 were detectable in 3 of 10 and 8 of 10, respectively, of the *gld/gld* animals analyzed after a single week of UV-B irradiation. FasL-deficient animals exposed to chronic UV-B irradiation for 2 weeks had p53 mutations in 4 of 10 and 6 of 10 in codons 270 and 275, respectively. No p53 mutations were detectable in nonirradiated wild-type or FasL-deficient mice. The infrequent p53 mutations in codons 270 and 275 in the epidermis of wild-type mice are in accordance with our previous report that such mutations are generally undetectable until 4 to 5 weeks after chronic UV-B exposure (*23*). The increase in p53 mutations in *gld/gld* mice exposed to UVR supports the hypothesis that FasL-induced apoptosis is required to efficiently eliminate DNA-damaged keratinocytes in the skin.

Cellular proofreading has been defined in p53-null mice where p53-dependent apoptotic pathways and DNA repair mechanisms are similarly compromised, rendering the relative importance of apoptosis for the elimination of DNA damage suspect if typical DNA repair pathways are intact (*2*, *3*). This work defines a critical role for apoptosis in cellular proofreading in the skin through FasL-Fas interactions. Circumvention of this apoptotic pathway, perhaps through a DNA damage threshold effect, may be essential for the survival of UVR-damaged cells containing mutations in critical regulatory genes. It is interesting to speculate that in surviving sun-damaged keratinocytes containing p53 mutations, consequent UVR-mediated DNA damage may not induce Fas expression (*9*, *10*) whereas FasL up-regulation would be likely retained (*7*). FasL expression in the absence of Fas-mediated apoptosis may confer a substantial advantage by immunologic privilege (*24*) allowing for the additional accumulation of DNA damage–induced mutations prerequisite for clonal expansion of the malignant cell.

UVR-induced FasL is the effector molecule mediating UVR-induced immune suppression (*25*), a process believed to be critical for the successful outgrowth of UVR-induced skin cancer in mice (*26*), and Fas loss of function results in the increased lung metastasis of UVR-induced murine melanomas (*27*). Taken together with the current findings, Fas and FasL interactions are likely pivotal in the etiology, growth, and metastasis of UVR-induced skin tumors.

References and Notes

1. H. S. Kahn, L. M. Tathum, A. V. Patel, M. J. Thun, C. W. Health, *J. Am. Med. Assoc.* **280**, 910 (1998).
2. A. Ziegler *et al.*, *Nature* **372**, 773 (1994).
3. D. E. Brash, *Nature Med.* **2**, 525 (1996).
4. G. Li, V. Tron, V. Ho, *J. Invest. Dermatol.* **110**, 72 (1998).
5. S. Nagata, *Cell* **88**, 355 (1997).
6. H. Chan, D. P. Bartos, L. B. Owen-Schaub, *Mol. Cell. Biol.* **19**, 2098 (1999).
7. S. Kasibhatla *et al.*, *Mol. Cell* **1**, 543 (1998).
8. C. Gutierrez-Steil *et al.*, *J. Clin. Invest.* **101**, 33 (1998).
9. P. Galle *et al.*, *J. Exp. Med.* **182**, 1223 (1995).
10. M. Muller *et al.*, *J. Clin. Invest.* **99**, 403 (1997).
11. M. Muller *et al.*, *J. Exp. Med.* **188**, 2033 (1998).
12. Specific pathogen-free C3H/HeJ mice were purchased from the National Cancer Institute–Frederick Cancer Research Facility Animal Production Area (Frederick, MD). C3H/HeJ *gld/gld* male mice were generated from a breeder colony maintained in our facility and housed in a pathogen-free barrier facility accredited by the Association for Assessment and Accreditation of Laboratory Animal Care in accordance with current U.S. Department of Agriculture, Department of Health and Human Services, and NIH regulations and standards. Animal procedures were approved by the Institutional Animal Care and Use Committee of the University of Texas M.D. Anderson Center. Mice were shaved and UV-irradiated as previously described (*23*). The UVR source was a bank of six Kodacel–(TA422 cellulose triacetate film, 127 μm thick; Eastman Kodak, Rochester, NY) filtered FS40 sunlamps (National Biological, Twinsberg, OH) that remove all UV wavelengths below 290 nm. The irradiance of the Kodacel-filtered sunlamps, measured with an IL-700 radiometer with an SE 240 UV-B detector, equipped with an A127 quartz diffuser (International Light, Newburyport, MA), averaged 5.22 W/m^2. The UV source was monitored weekly by placing the UV-B detector in a cage equipped with a wire top. Under these conditions, mice were exposed to UV-B radiation (2.5 W/m^2). For all experiments, mice were exposed to single or multiple doses of UV-B (5 kJ/m^2) corresponding to 2.3 minimal erythemal doses for C3H mice.
13. Formaldehyde-fixed skin biopsies were paraffin-embedded, and immunohistochemistry was performed as previously described (*27*) with polyclonal goat antibody to Fas (X-20), FasL (M-20) (Santa Cruz Biotechnology, Santa Cruz, CA), or normal goat serum (isotype control) at final dilutions of 1:500. Staining was visualized with stable diaminobenzidine (Research Genetics, Huntsville, AL). Specificity of staining was confirmed with blocking peptides; preincubation of antibody with specific peptide eliminated all staining. FasL staining was also verified with a monoclonal antibody to FasL (KAY-10; Pharmingen).
14. Shaved dorsal skins were fixed in buffered 10% formalin and embedded in paraffin. Five-micrometer sections were stained with hematoxylin-eosin and examined by light microscopy. Criteria for scoring sunburn cells were intensely staining eosinophilic cytoplasm, pycnotic nuclei, and separation from adjacent cells as previously described (*2*). For each of two to five mice per point, 10 hematoxylin-eosin sections from two separate epidermal sections were counted for sunburn cells. Sunburn cell incidence was calculated per linear centimeter of epidermis with coded slides that did not reveal treatment group. No detectable differences between wild-type and *gld/gld* mice in morphology, organization, or thickness were observed in the epidermis.
15. Dorsal skins were fixed in buffered 10% formalin and embedded in paraffin. TUNEL assay was done with a commercially available kit according to the manufacturer's directions (Promega, Madison, WI). Slides were examined with an Olympus Inverted System Microscope IX70 (Melville, NY), and pictures were taken with a Nikon 35-mm camera (magnification, ×10).
16. L. L. Hill *et al.*, data not shown.
17. Data can be accessed at www.sciencemag.org/feature/data/1040041.shl
18. L. L. Hill and L. B. Owen-Schaub, unpublished observations.
19. A. S. Jonason *et al.*, *Proc. Natl. Acad. Sci. U.S.A.* **93**, 14025 (1996).
20. S. Kanjilal, W. E. Pierceall, K. K. Cummings, M. L. Kripke, H. N. Ananthaswamy, *Cancer Res.* **53**, 2961 (1993).
21. H. N. Ananthaswamy *et al.*, *Photochem. Photobiol.* **67**, 227 (1998).
22. Epidermis from ~8-cm^2 pieces of dorsal skin from the midline of each mouse was separated from the dermis by floating the skin dermis side down in phosphate-buffered saline containing 0.25% trypsin for 2 hours at 37°C followed by mechanical separation and freezing of epidermis. Frozen epidermis was digested in lysis buffer [4 M urea, 0.5% *N*-lauroylsarcosine, 10 mM EDTA, 0.2 M NaCl, and 100 mM tris-HCl (pH 8.0)] containing proteinase K (300 μg/ml) and ribonuclease (100 μg/ml) at 37°C overnight. Samples were heated at 60° for 15 min, and the DNA was extracted with the phenol-chloroform method. The primer sequences used were as follows: codon 270, 5′-GGACGGGACAGCTTTGAGGTTT-3′ (forward); codon 275, 5′-GTGTTTGTGCCTGCCT-3′ (forward); and 3′ prime end of exon 8, 5′-GCCTGCGTACCTCTCTTTGC-3′. The PCR product was resolved on a 6% polyacrylamide gel and visualized on autoradiographic film.
23. H. N. Ananthaswamy *et al.*, *Nature Med.* **3**, 510 (1997).
24. T. S. Griffith, T. Brunner, S. M. Fletcher, D. R. Green, T. A. Ferguson, *Science* **270**, 1189 (1995).
25. L. L. Hill, V. K. Shreedhar, M. L. Kripke, L. B. Owen-Schaub, *J. Exp. Med.* **189**, 1275 (1999).
26. M. S. Fisher and M. L. Kripke, *Science* **216**, 1133 (1982).
27. L. B. Owen-Schaub, K. L. van Golen, L. L. Hill, J. E. Price, *J. Exp. Med.* **188**, 1717 (1998).

28. We thank L. Eichler for expert technical assistance and M. Duvic and D. McConkey for critical review of this manuscript. This work was supported by grants from the Skin Cancer Foundation, American Cancer Society (CIM-96070 to L.O.-S.), and NIH (CA45623 to H.N.A. and CA52457 to L.O-S.). L.L.H. is the recipient of the Crockrell University Cancer Fighters Scientific Achievement Award and an NIH postdoctoral fellowship (F32 AI09351).

15 March 1999; accepted 7 July 1999